

# Segmentation of welding defects using a robust algorithm

Miguel Carrasco<sup>1</sup> and Domingo Mery<sup>2\*</sup>

<sup>1</sup>Departamento de Ingeniería Informática  
Universidad de Santiago de Chile  
Email: miguel.carrasco@usach.cl

\* Corresponding author  
<sup>2</sup>Departamento de Ciencia de la Computación  
Pontificia Universidad Católica de Chile  
Email: dmery@icee.org

## Abstract

This work presents a new method capable of segmenting welding defects using robust digital image processing techniques, within which are included noise attenuation filters, morphological mathematical operators, edge detection techniques such as the Canny filter, the Watershed transform, and the distance transform. In order to determine the quality of the segmentation generated by the algorithm, the segmented image is compared with an ideal binary image developed manually. The results of this study have led to the development of the following scheme: first a median filter is used for noise reduction; second, a bottom-hat filter is used to separate hypothetical flaws from their background; third, the segmented regions are identified by means of binary thresholding; fourth, filters taken from morphological mathematics are used to eliminate over-segmentation; and fifth the Watershed transform is used to separate internal regions. The results of the study have generated an area underneath the ROC curve of 0.9358 in a set of ten images. The best operational point reached corresponds to an 87.83% sensitivity and a 9.40% of 1-specificity.

**Keywords:** X-ray testing, welding inspection, digital image processing, automatic defect detection.

## 1 Introduction

Computer vision is a key factor for the implementation of total quality within the different processes in industrial automation. Companies that use this technology acquire a competitive advantage because it leads to increased production, an improvement in the quality of products, and a decrease in manufacturing costs as well, (González, 1992).

The process that allows automated computer vision is known as Automatic Visual Inspection (AVI), and its objective is to determine whether a product lies inside or outside the range of acceptance for a determined manufacturing process. To this end, different techniques for digital image processing are used (Newman & Jain, 1995). AVI is a denomination that encompasses a large group of analyses and algorithms that are divided by a series of processing

stages among which are; image formation, pre-processing, segmentation, extraction of characteristics and classification.

One of the principal avenues of research in AVI is the process of automatic flaw recognition because automation allows the setting of policies and precise and objective control protocols, whereas manual systems are subject to weariness and routine on the part of the operator, which may lead to a deficient or inconstant control. There are two basic conditions that an AVI system must meet in order to improve product quality; the first is efficiency or ensuring the least possible number of false positives and negatives; the second is speed, i.e. the production process should not be affected by the time required for inspection and thus production should either increase or at least maintain speed.

Segmentation is one of the initial stages within the AVI process. Its application allows the initial separation of regions of interest which are subsequently classified. Segmentation is often considered the most complex task in the processing of images (González, 1992). Research in this area is copious but specific to the material being analyzed. In the case of the present investigation, different strategies and methods have been evaluated that centre on the detection of flaws in welding images.

This article is organized as follows: Section 2 present the state of the art in flaw detection in welds. Section 3 presents the segmentation methods and the solution scheme developed in this study. Section 4 presents the results obtained. Lastly, Section 5 presents our conclusions. An extended version of this article may be found in (Carrasco, 2004).

## **2 State of the Art**

There are structures that use welds for critical functions, such as high pressure equipment, chemical compounds, etc, where any kind of flaw can trigger catastrophic consequences. Because of this, there are conventional forms for detecting welding flaws by means of visual inspection of radiographic images. These images are generated by means of X-rays and  $\gamma$ -rays which penetrate the material generating a radiological image on a photographic plate. Flaws are detected due to variations in the density of the material (see Figure 1). Nonetheless, manual interpretation of flaws generates subjective and imprecise results which require a great deal of time and are inconsistent in that they depend on an inspector for their analysis (Liao, 2003).

Due to the problems associated with manual detection, there is currently a great deal of work and research on non-destructive testing (NDT) methods for detecting welding defects. The objective is to develop an automated method for the detection of defects that is precise and objective. Some of the most important achievements in this area are presented below.

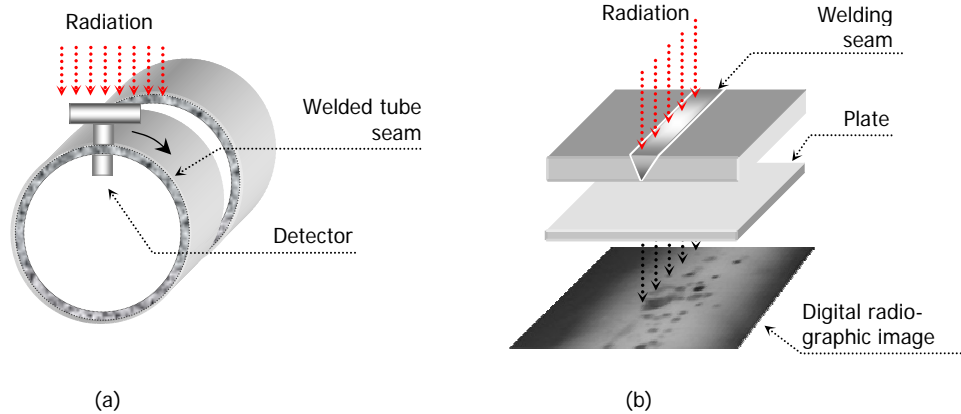


Figure 1. (a) Flaw detection scheme through radiation of weld, (b) Radiation over material flaw captured on a radiographic plate.

Gayer et al, (1990) proposed a method that can be summarized as having two steps: i) A quick search for potential defects in the X-ray image: Assuming that the defects will be smaller than the regular structure of the test piece, potential defects are classified as those regions of the image where higher frequencies are significant. The spectrum of the X-ray image is determined with the help of a fast Fourier transformation, which is calculated either row by row or column by column in small  $32 \times 32$  windows. When the sum of the higher frequencies of a window is greater than a given threshold value, the entire window is marked as potentially defective. Another possibility is suggested by the authors as part of this task: A window is selected as potentially defective when the sum of the first derivative of the rows and columns of a window is large enough. ii) Identification and location of the true defect: Because of the time-consuming nature of this step, only those regions which were previously classified as being potentially defective are studied here. Two algorithms were developed here as well. The first leads to a matching<sup>1</sup> between the potential defect and typical defects, which are stored in a library as templates. Whenever a large resemblance between the potential defect and a template is found, the potential defect is classified as a true defect. The second algorithm estimates a defect-free X-ray image of the test piece by modelling every line of an interpolated spline function without special consideration for the potentially defective region. Following this, the original and the defect-free images are compared. True defects are identified when large differences occur compared to the original input image.

In 1994 Lawson and Parker proposed in (Lawson & Parker, 1994) that artificial neural networks (ANN) be used for the automated detection of defects in X-ray images. The method generates a binary image from the test image where each pixel is either 0 when a regular structure feature of the piece or 1 when a defect is detected. This entails the supervised learning of a multi-layer perceptron network (MLP) where the attempt is made to obtain detection from training data. A back propagation algorithm is used for the assignment of weightings within the MLP. The authors use one of two hidden layers in the network topography of the ANN, where the input signal corresponds to a window of  $m \times m$  grey values in the X-ray image. The output signal is the pixel at the image centre in the binary image. Since the threshold value function for the neurons are sigmoidal in this method, a threshold is used to obtain a binary output signal.

<sup>1</sup> Matching is performed with a Sequential Similarity Detection method.

The desired detection in the training data was obtained with a segmenting procedure based on an adaptive threshold. During the experiments of five X-ray images, Lawson and Parker show that the detection using ANN is superior to the segmenting method using adapted thresholds.

A method for automated recognition of welding defects was presented in (Sofia & Redouane, 2002). The detection follows a pattern recognition methodology: i) Segmentation: regions of pixels are found and isolated from the rest of the X-ray image using a watershed algorithm and morphological operations (erosion and dilation). ii) Feature extraction: the regions are measured and shape characteristics (diameter variation and main direction of inertia based on invariant moments) are quantified. iii) Classification: the extracted features of each region are analyzed and classified using a  $k$ -nearest neighbour classifier. According to the authors, the method is robust and achieves a good detection rate.

In (Silva et al, 2002) a welding defect classification method is proposed. In a first step, called image pre-processing, the quality of the X-ray image is improved using a median filter and a contrast enhancement technique. The defect detection follows the pattern recognition schema mentioned above: i) Potential defects are segmented in the X-ray image. ii) Geometric and grey value features (contrast ( $C$ ), position ( $P$ ), aspect ratio ( $a$ ), width-area ratio ( $e/A$ ), length-area ratio ( $L/A$ ) and roundness( $R$ )) are extracted. The correlation between features and each considered defect class (slag inclusion, porosity, lack of penetration and undercutting) was evaluated by analyzing the linear correlation coefficient. iii) The most relevant features were used as input data on a hierarchic linear classifier (Silva et al, 2001). In order to achieve a higher degree of reliability for the results, radiographic standards from the International Institute of Welding were used, with 86 films containing the main defect classes. The experimental results show that the features  $P$  and  $e/A$  are able to classify the undercutting and lack of penetration classes. Nevertheless, the six mentioned features are required to obtain a high performance by classifying the porosity and inclusion defects.

Liao and Li (1998) propose a detection approach based on a curve fitting. The key idea of this work is to simulate a 2D background for a normal welding bead characterized by low spatial frequencies in comparison with the high spatial frequencies of defect images. Thus, a 2D background is estimated by fitting each vertical line of the weld to a polynomial function, and the obtained image is subtracted from the original image. The defects are detected where the difference is considerable. Wang & Liao (2002) and Liao (2003) propose a fuzzy  $k$ -nearest neighbour, multi-layer perceptron neural network and a fuzzy expert system for the classification of welding defect types. The features used for the classification are distance from centre, circularities, compactness, major axis, width and length, elongation, Heywood diameter and average intensity and standard deviation of intensity. Finally the (K-NN) and the (MLP) methods are used for classification. The results indicate that the (MLP) method is superior to the (K-NN) method, classifying 92.39% and 91.57% respectively.

In 2003, Mery and Berti (Mery & Berti, 2003), presented a new methodology based on texture analysis. Texture is one of the most important characteristics in pattern recognition, however it has seen limited use in the analysis of digital images in NDT. The referenced study examines the analysis of two types of texture features: those based on the occurrence matrix, and those based on the Gabor function. The proposed approximation uses the following methodology: i) Segmentation: the LoG edge detector is used, ii) Extraction of characteristics: the features of potential defects are extracted, iii) Classification: the most relevant features are used as input

data for a statistical classifier. The best results have been achieved with a polynomial classifier, with a 91% defect detection, and 8% false alarm rate.

The literature reviewed includes a large quantity and variety of methodologies for the detection of welding defects, such as interpolating the image's background curves, neuronal networks, geometric characteristics, application of mathematical morphology and the Watershed algorithm, texture analysis, etc. Research in this area continues largely because there are, as of yet, no satisfactory results that allow the detection of the totality of flaws without false alarms. Additionally, it is not possible to determine which of the lines of investigation will improve the overall result, because each of them has room for improvement. The research presented in the present work is justified as it develops a new segmentation method which improves the process of automated detection of welding defects. Moreover, it is also dedicated to developing a methodology that gathers some of the best characteristics of the reviewed studies such as the application of a median filter (Silva et al, 2002), the comparison between a real image and a defect free image (Liao & Li, 1998), the use of mathematical morphology, and the Watershed algorithm (Sofia & Redouane, 2002).

### **3 Proposed Segmenting Methods.**

Segmentation consists of partitioning the image into disjoint regions, where each region is homogenous with respect to a given property, such as texture, grey level, type of colour, etc. with the purpose of separating regions of interest for their posterior recognition (González, 1992). Thus, the segmentation problem can be approached with different methods, which generally can be categorized into three types of techniques; those oriented towards the detection of edges, pixel detection, and region detection (Castleman, 1996).

In our study, the edge detection was firstly performed using gradient approaches. The Roberts, Prewitt, Sobel and Laplace of Gaussian (Castleman, 1996) filters belong to this category. These calculate the gradient and according to some threshold level determine if a possible edge exists. Subsequently the Canny filter (Canny, 1986) was reviewed. This filter uses a combination of techniques, such as the Gaussian Filter for the elimination of noise, as well as making use of directional gradients, thus allowing the selection of only those edges that are found within the specified threshold. In pixel detection we have thresholding (Castleman, 1996) which is a widespread technique as it allows the conversions of an image in grey scale to a binary image in such a way as to separate background objects according to a specified threshold. The Watershed transform (Beucer et al, 1979) is used in region detection. This technique makes use of morphological mathematics and allows the generation of regions based on cavity filling, simulating a valley filling with water; in the measure that the water level rises, adjacent regions start forming unions. Additionally, we also studied the distance transform (Breu et al, 1995) and the manner in which it can improve segmentation quality by using the Watershed transform.

In this case segmentation is used with the purpose of separating known regions from "hypothetical defects". These regions are made up of true defects as well as false alarms, and it is the task of the classifier to correctly separate these two groups according to a set of geometric properties such as: area, perimeter, invariant moments, etc. which are analyzed in the characteristic extraction process (Mery & Filbert, 2002).

The proposed segmentation process uses a combination of digital processing techniques which have been selected on the basis of experimental tests and analyses, the development of which is presented in Figure 2. Each stage has been analyzed independently and globally which has allowed the study of different variations and strategies. Among the variants related to noise, the Gaussian filter and the mean filter were studied. It was shown that the median filter lowers noise levels without affecting the quality of the edges.

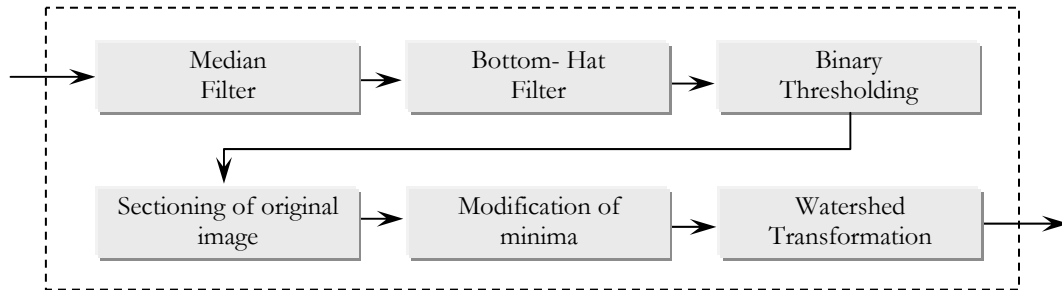


Figure 2. Proposed segmentation process

Moreover, a bottom-hat filter has allowed identification of the majority of the defects by separating them from the background. This filter is made up of two stages: first a morphological closure operator is used on the original image which allows the generation of a background image similar to the original but without flaws. In the second stage, the subtraction operator is used on the original image and the image produced in the first stage (Mathworks, 2003). To a large extent this characteristic determines the quality of the segmentation by analyzing the hypothetical defects. In the edge detection process, the binary thresholding method has been selected as it allows the obtainment of closed structures, and only requires a noise elimination process through the closure. On the other hand, we showed the difficulty encountered by the Canny method in closing edges by means of morphological methods. Later, in the sectioning process, the advantages of copying the regions of the original image have been shown when compared to the distance transform as the latter only simulates the defect structures, whereas if the original image's pixels are used, a much more precise segmentation is obtained.

The modification of minima is part of the strategy named "*Homotopy modification*" (Beucher, 1991), which has allowed the avoidance of over-segmentation, and the generation of a more precise segmentation. However, it is important to determine the number of pixels that make up the minimum because a variation in this figure can generate a greater or smaller number of hypothetical flaws. The final tool employed is the Watershed transform. This technique, in combination with the modification of minima, allows the segmentation of structures in the interior of the structure because the external segmentation has been carried out previously in the process of binary thresholding. The general segmentation process, especially the stage of binary thresholding has facilitated the generation of the majority of the structures and their edges. It has been shown that the Watershed transform by itself does not generate the segmentation of the defects as it segments the entire image, thus highlighting the importance of step previous to its application. An example of the proposed segmentation process is presented in Figure 3 in a portion of the BAM-5 image.

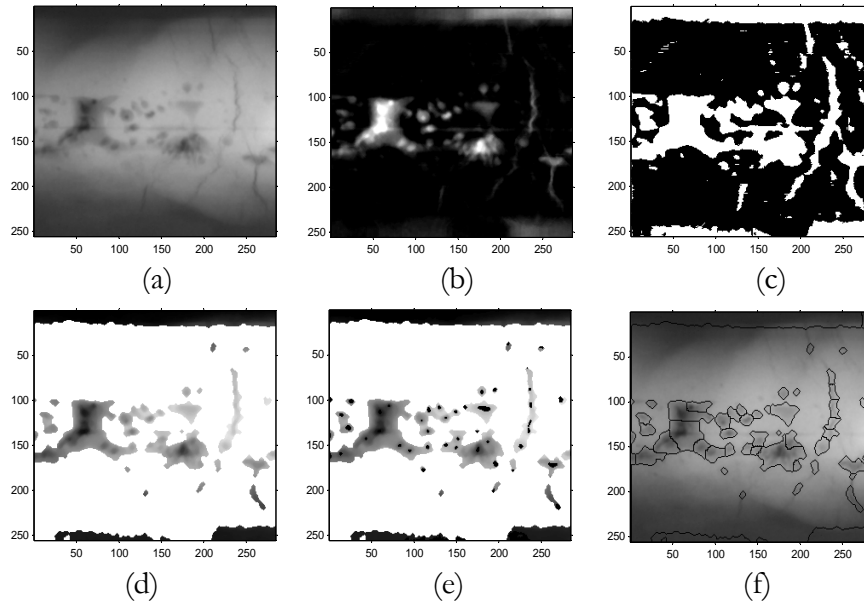


Figure 3. Summary of the proposed segmentation process (a) Image alter the application of the median filter, (b) Application of the Bottom-Hat filter, (c) Application of binary thresholding, (d) Application sectioning process, (e) Modification of minima (f) Application of the Watershed transformation.

Figure 4 shows the effects of applying a threshold to the segmentation process. As the threshold is increased the segmented regions diminish, and moreover they tend to have a lesser internal area. Other process variables, such as the bottom-hat filter, cut-off point selection and dilation and erosion operations, influence in the quantity and form of the regions. Nonetheless, modifying the variables generates different results, in some cases this change can result in imprecise segmentation, and thus it is important to analyze the effect resulting from the modification of each variable, and how it affects the final result.

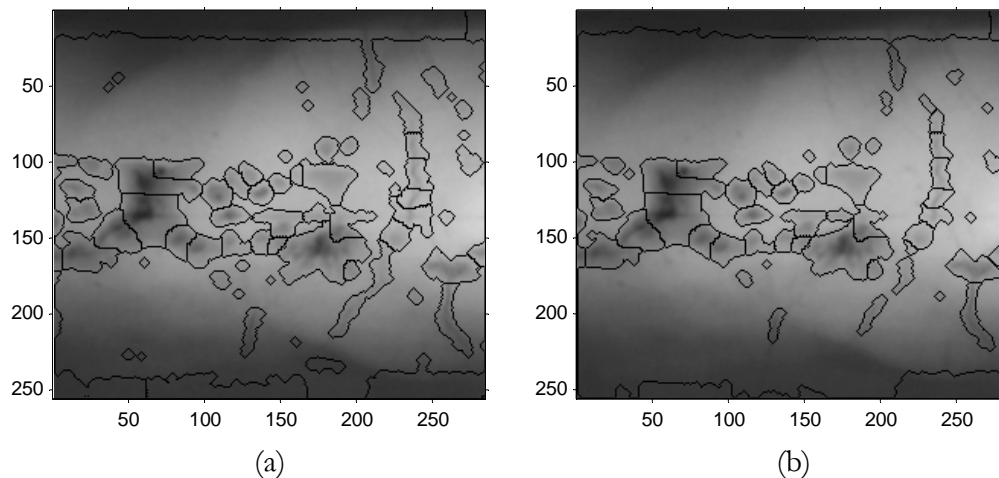


Figure 4. (a) Segmentation of the image with threshold = 3, (b) Segmentation of the image with threshold = 5.

## 4 Results

The ROC (receiver operation characteristic) analysis is commonly used to measure the performance of a two-class classification. In our case, each feature is analyzed independently using a threshold classifier. This way, a hypothetical flaw is classified as a 'no-defect' (or 'defect') if the value of the feature is below (or above) a threshold value. The ROC curve represents a 'sensitivity' ( $S_n$ ) versus '1-specificity' ( $1-S_p$ ), defined as:

$$S_n = \frac{TP}{TP + FN}, \quad 1 - S_p = \frac{FP}{TN + FP}$$

in which  $TP$  is the number of true positives (correctly detected defects),  $TN$  is the number of true negatives (correctly detected no-defects),  $FP$  is the number of false positives (false alarms, or no-defects detected as defects) and  $FN$  false negatives (flaws detected as no-defects). Ideally,  $S_n = 1$  and  $1-S_p = 0$ , this means that all defects were found without any false alarms. The ROC curve makes it possible to evaluate the performance of the detection process at different points of operation (as defined for example by means of classification thresholds). The area under the curve ( $A_c$ ) is normally used as a measure of this performance as it indicates how flaw detection can be carried out: a value of  $A_c = 1$  indicates an ideal detection, while a value of  $A_c = 0.5$  corresponds to random classification (Duda et al, 2001).

The analysis of the ROC curve is carried out according to the method proposed in (Mery & Pedreschi, 2003). For each image, an ideal detection was achieved using visual interpretation. The methodology was to create an ideal binary image ('1' is defect and '0' is non-defect) according to the visual information with the software Microsoft Paint using the biggest scale (zoom = 800%). The results obtained with our algorithm were then compared with the ideal binary image. Thus, the values for  $TP$ ,  $TN$ ,  $FP$  and  $FN$  were tabulated according to Figure 5.

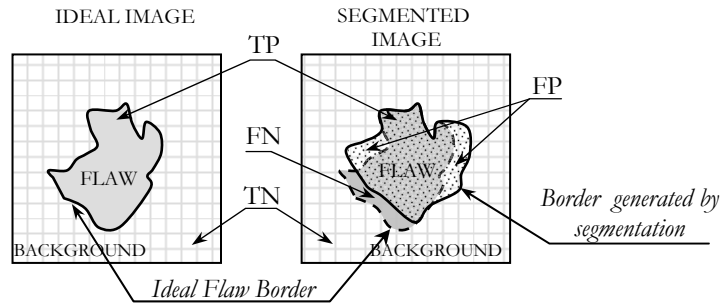


Figure 5. Representation of the differences between the ideal and segmented image

Table 1 presents a summary of the images analyzed in this study. The column labelled "Number of ideal regions" presents the number of real regions that must be segmented. The sensitivity and 1-specificity analysis is carried out pixel by pixel using the method proposed in (Mery & Pedreschi, 2003). For this reason, the results differ from the results presented in (Mery & Berti, 2003), in which regions are analyzed as sets, and not pixel by pixel.

Table 1. Summary of the segmented images and their best sensitivity and 1-specificity values.

#	Image Name	Image size in pixels	Number r of ideal regions	Regions segmented by the process	Best operational points		$A_z$
					Sensitivity	1- Specificity	
1	BAM5.tif	3512x366	273	495	90.04%	7.62%	93.08%
2	12R_M.tif	4919x835	36	933	96.93%	3.87%	98.03%
3	13R_M.tif	4125x686	62	520	90.38%	7.47%	95.22%
4	22R_M.tif	4992x646	23	678	94.21%	4.29%	97.44%
5	28R_M.tif	4968x527	47	1062	91.08%	5.10%	94.34%
6	31R_M.tif	4968x756	11	179	99.51%	0.58%	99.52%
7	39R_M.tif	4973x745	90	1110	87.68%	7.86%	94.36%
8	40R_M.tif	4964x775	30	731	82.28%	3.74%	91.31%
9	106R_M.tif	4981x494	97	836	81.24%	6.17%	89.90%
10	107R_M.tif	4953x1091	59	2461	80.65%	10.96%	89.41%

The images used correspond to 10 of the images catalogued by BAM<sup>2</sup> for non-destructive testing in welding seams. These have been captured using a Lumysis scanner LS85 SDR, in high density mode. An LUT linear fit has been used in order to reduce the grey levels of the original images from 12 to 8 bits. Additionally, they have been resized to leave only those areas that must be segmented.

In order that the study of the images do not depend on the set analyzed, a generalized ROC curve has been developed. This curve incorporates tests that use the same values with the purpose of obtaining a set of optimum parameters that will allow the use of this filter on an image that is not part of the study. In order to calculate the curve presented in Figure 6 the values for *TP*, *FN*, *FP* and *TN* have been added for each test in the study, taking into account that the values being summed must be generated on the basis of the same test for each image. Subsequently the ‘sensitivity’ and ‘1-specificity’ values are calculated.

The ROC curve in Figure 6 has an area of 93.58%; its best point has an 87.83% sensitivity and a 9.40% 1-specificity. The next-best point has a 86.72% sensitivity and a 7.98% 1-specificity. In this latter case the decrease in false alarms is due to the increase in the area of detection which means that regions with less than 27 pixels are not considered as ‘hypothetical flaws.’

The proposed filter has been compared with the method developed in (Mery & Berti, 2003). In order to carry out the comparison a binary image has been generated manually which contains all the real flaws of the original image. Once the segmented regions have been determined with the use of the proposed filter and the texture analysis filter, the results can be compared against the ideal binary image.

<sup>2</sup> BAM, Federal Institute for Materials Research and Testing, Berlin.

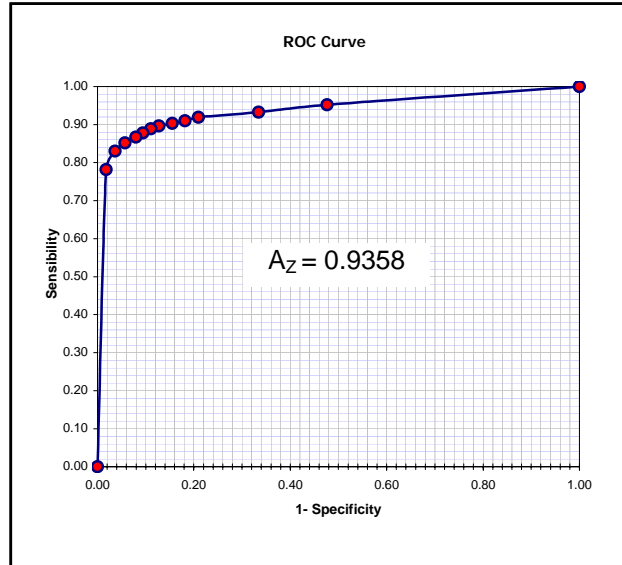


Figure 6. ROC Curve for  $TP$ ,  $FN$ ,  $FP$ , and  $TN$  values determined from a set of tests with the same parameters.

Table 2. Comparison between the developed filter and the texture analysis filter for the BAM-5 image

IMAGE	PROCESS	SEGMENTED REGIONS	CLASSIFIED REGIONS	SENSITIVITY	1-SPECIFICITY
Bam5.tif	Bottom-hat segmentation (proposed filter)	495	---	90.04%	7.62%
Bam5.tif	Texture Analysis (Mery & Berti, 2003)	1419	187	64.13%	4.86%

As can be seen in Table 2, the results show that the sensitivity for the method developed in this investigation is 90.94% compared with 64.13% for the texture analysis method. Additionally, the 1-specificity is 7.62% compared to 4.86% for the texture analysis method. This shows that the proposed method detects a greater number of false alarms, but at the same time detects a greater number of real flaws.

The purpose behind having a smaller number of segmented regions is to reduce processing time for the latter stages of AVI. The type of region being analyzed is important for the process, and consequently two objectives must be met: decrease the number of segmented regions while simultaneously having a low number of false alarms. To this end the segmentation process must be as precise as possible in detecting real defects.

These results indicate that the proposed filter has two advantages: the first is a reduction in the number of regions which implies that during subsequent characteristic-extraction and classification processes, fewer regions need analyzing, which reduces processing time. The second advantage consists in having a high percentage of regions with real flaws and a low percentage of false alarms. This implies that when the segmentation process is applied, the majority of real flaws are included.

## 5 Conclusions

One of the principal filters used in the detection of hypothetical flaws is the bottom-hat filter. Should the flaw have a minimum of contrast with the background, this filter will not detect it. Noise plays an important role in the result of segmentation because if it is too high, a larger mask must be applied, and thus low intensity flaws disappear. On the other hand if a smaller mask is used, a large number of regions will be generated which will, for the most part, correspond to noise regions.

The analysis of the results indicates that the proposed filter is sensitive to noise; as noise increases, a larger number of regions is detected, when noise decreases fewer regions are segmented. This effect can be minimized by using a median filter because of its noise attenuating properties and preservation of the structure of edges.

This work has effected a comparison with the method developed in (Mery & Berti, 2003). This latter method carries out segmentation by means of the LoG filter, extraction is carried out through the co-occurrence matrix and the Gabor function, and finally the classification process is implemented through the use of the polynomial, Mahalanobis and near-neighbour methods. Clearly the comparison with the proposed filter is not entirely fair, as only the segmentation process has been carried out. However, the results may improve on application of the next stages of AVI such as the extraction of characteristics and classification. The results indicate that the sensitivity of the proposed method is of 90.94% compared to 64.13% for the texture analysis method. Additionally, the 1-specificity is 7.62% compared to 4.86% respectively.

## 6 Acknowledgments

The authors wish to thank the Federal Institute for Materials Research and Testing, Berlin (BAM) for the radiographic material used in this investigation. This work was supported in part by Fondecyt Project Number 1040210.

## 7 References

1. BEUCHER, S.; LANTUÉJOL, C.: "Use of Watersheds in Contour Detection". Proc. Int. Workshop on image processing, Rennes, France, September, 1979, pp. 17-21.
2. BEUCHER S.: "The Watershed Transformation applied to Image Segmentation", 10th Pfefferkorn Conf. on Signal and Image Processing in Microscopy and Microanalysis, 16-19 September, 1991.
3. BREU, H.; GIL, J.; KIRKPATRICK, D.; WERMAN, M.: "Linear Time Euclidean Distance Transform Algorithms", IEEE Transactions on Pattern Analysis and Machine Intelligence, vol. 17, no. 5 May, 1995, pp. 529-533.
4. CARRASCO, M.: "Segmentation of welding defects using digital image processing techniques" (in Spanish). Master of Science Thesis, Departamento de Ingeniería Informática, Universidad de Santiago de Chile, Abril, 2004.
5. CANNY, J.: "A Computational Approach to Edge Detection". IEEE Trans. Pattern Analysis and Machine Intelligence, 1986, PAMI-8:(6), 679-698.
6. CASTLEMAN, K.R.: "Digital Image Processing". Prentice-Hall, New Jersey, 1996.
7. DUDA, R., HART, P., STORK, D.: "Pattern Classification". 2 edn. John Wiley & Sons, Inc., New York 2001

8. GAYER, A.; SAYA, A.; SHILOH, A.: "Automatic recognition of welding defects in real-time radiography". *NDT International*, 23(4):131–136.
9. GONZÁLEZ R.; R.E. WOODS: "Digital Image Processing", Addison Wesley, 1992, U.S.A.
10. LAWSON, S.; W, PARKER G. A.: "Intelligent segmentation of industrial radiographic images using neural networks". In *Machine Vision Applications and Systems Integration III*, Proc. of SPIE, volume 2347, pages 245–255, November 1994.
11. LIAO, T W, LI, Y M.: "Weld defect detection based on Gaussian Curve". *Proceedings of the 28th Southeastern Symposium on System Theory (SSST '96)*
12. LIAO, T W, LI, Y M.: "An Automated Radiographic NDT System for Weld Inspection", Part II – Flaw detection. *NDT&E International*, 31(3):183-192., 1998.
13. LIAO; T.W.: "Classification of welding flaw types with fuzzy expert systems", *Expert Systems with Applications* 25, 101–111, 2003.
14. MATHWORKS; "Image Processing Toolbox for Use with MATLAB: Users Guide". The MathWorks Inc., Enero 2003.
15. MERY, D.; FILBERT D.: "Automated Flaw Detection in Aluminum Castings Based on the Tracking of Potential Defects in a Radioscopic Image Sequence". *IEEE Transactions on Robotics and Automation*, 18(6): 890-901, 2002. ISSN 1042-296X.
16. MERY, D.; BERTI, .M.A.: "Automatic Detection of Welding Defects using Texture Features. *Insight*, 45(10):676-681, 2003. ISSN 1354-2575, 2003.
17. MERY, D.; PESDRESCHI F.: "Segmentation of colour food images using a robust algorithm", *Journal of Food Engineering* (in Press).
18. NEWMAN, T.S.; JAIN, A.K.: "A survey of automated visual inspection", *Computer Vision and Image Understanding*, 61(2):231-262, 1995.
19. SILVA, R R, SIQUEIRA, M H S, CALÓBA, L P, DA SILVA, I C, DE CARVALHO, A A, REBELLO, J M A. (2002). "Contribution to the development of a radiographic inspection automated system". In *Proceedings of the 8th European Conference on Non-Destructive Testing (ECNDT 2002)*, Barcelona, 17-21 June 2002.
20. SOFIA, M.; REDOUANE, D.: "Shapes recognition system applied to the non destructive testing". In *Proceedings of the 8th European Conference on Non-Destructive Testing (ECNDT 2002)*, Barcelona, 17-21 June 2002.
21. WANG, G, LIAO, W.: "Automatic Identification of different types of welding defects in radiographic images". *NDT&E International*, 35(2002):519-528.